

Sr₃Sc₂Fe₂As₂O₅ as a possible parent compound for FeAs-based superconductors

Xiyu Zhu, Fei Han, Gang Mu, Bin Zeng, Peng Cheng, Bing Shen, and Hai-Hu Wen*

*Institute of Physics and Beijing National Laboratory for Condensed Matter Physics,
Chinese Academy of Sciences, P.O. Box 603, Beijing 100190, China*

(Received 13 November 2008; revised manuscript received 16 December 2008; published 23 January 2009)

A compound with the FeAs-layers, namely, (Sr₃Sc₂O₅)Fe₂As₂ (abbreviated as FeAs-32522), was successfully fabricated. It has a layered structure with the space group of *I4/mmm*, and with the lattice constants $a = 4.069$ Å and $c = 26.876$ Å. The in-plane Fe ions construct a square lattice which is close to that of other FeAs-based superconductors, such as REFeAsO (RE=rare earth elements) and (Ba,Sr)Fe₂As₂. However the inter-FeAs-layer spacing in the compound is greatly enlarged. The temperature dependence of resistivity exhibits a weak upturn in the low-temperature region, but a metallic behavior was observed above about 60 K. The magnetic susceptibility shows also a nonmonotonic behavior. Interestingly, the well-known resistivity anomaly which was discovered in all other parent compounds, such as REFeAsO, (Ba,Sr)Fe₂As₂ and (Sr,Ca,Eu)FeAsF and associated with the spin-density wave/structural transition has not been found in the new system either on the resistivity data or the magnetization data. This could be induced by the large spacing distance between the FeAs-planes, therefore the antiferromagnetic correlation between the moments of Fe ions in neighboring FeAs layers cannot be established. Alternatively it can also be attributed to the self-doping effect between Fe and Sc ions. The Hall coefficient R_H is negative but strongly temperature dependent in wide temperature region, which indicates the dominance of electrical conduction by electronlike charge carriers and probably a multiband effect or a spin related scattering effect. It is found that the magnetoresistance cannot be described by Kohler's rule, which gives further support to above arguments.

DOI: [10.1103/PhysRevB.79.024516](https://doi.org/10.1103/PhysRevB.79.024516)

PACS number(s): 74.70.Dd, 74.25.Fy, 75.30.Fv, 74.10.+v

I. INTRODUCTION

Superconductivity in the FeAs-based systems has received tremendous attention in last several months with the hope that the superconducting transition temperature could be raised to a higher value.¹ Experimentally, it has been found that the highest T_c is about 55–57 K in the fluorine doped REFeAsO compound^{2,3} or RE doped (Ca,Sr)FeAsF (RE=rare earth elements).⁴ Meanwhile the family of the FeAs-based superconductors has been expanded rapidly. In the system of (Ba,Sr)_{1-x}K_xFe₂As₂ (denoted as FeAs-122), the maximum T_c at about 38 K was discovered.⁵⁻⁷ In the Li_xFeAs (denoted as FeAs-111) system, superconductivity at about 18 K was found.⁸⁻¹⁰ In the material FeSe_{1-x} which has no toxic arsenic and a more simple structure,¹¹ it was shown that the sample became superconductive at about 8 K. By doping or using a high pressure, the T_c can be pushed higher. Superconductivity at about 2.2 K has also been found in a NiP-based layered structure La₃Ni₄O₂P₄ with the intergrowth of NiP-1111 and 122 building blocks.¹² Very recently, another kind of parent compounds (Sr,Ca,Eu)FeAsF were reported,¹³⁻¹⁶ which may lead to high-temperature superconductors by doping charges into the system.

Empirically it is found that the superconducting transition temperature rises when the inter-FeAs-layer spacing distance d_{FeAs} is increased (F-SmFeAsO: $T_c = 55$ K, $d_{\text{FeAs}} = 8.7$ Å; (Sr,Ba)_{1-x}K_xFe₂As₂: $T_c = 38$ K, $d_{\text{FeAs}} = 6.5$ Å; Li_xFeAs: $T_c = 18$ K, $d_{\text{FeAs}} = 6.4$ Å) in the FeAs-based superconductors. Surprisingly this seems to be quite similar to the case in the cuprates. For example, by using the effective layers of CuO planes in the cuprates, superconductors with different structures were discovered. They can be categorized into the so-called single-layer systems La_{1-x}Sr_xCuO₄ and Bi₂Sr₂CuO₆

with the maximum T_c of about 38 K, or the double-layer systems YBa₂Cu₃O₇ and Bi₂Sr₂CaCu₂O₈ with the optimal T_c of about 85–92 K, or the triple-layer system Bi₂Sr₂Ca₂Cu₃O₁₀ with the maximum T_c of about 123 K (at ambient pressure).¹⁷ As inspired by the experience in the cuprate superconductors, a larger separation between the superconducting planes (here the FeAs layers) may lead to a higher T_c . Thus it becomes very interesting to see whether it is possible to fabricate a compound with larger spacing distance between the FeAs planes. In this paper, we report the discovery of another kind of FeAs-based layered compound (Sr₃Sc₂O₅)Fe₂As₂ (abbreviated as FeAs-32522), which has an inter FeAs-layer spacing distance of about 13.438 Å, being much larger than those in all other parent compounds discovered so far, such as REFeAsO, FeAs-122, and (Sr,Ca,Eu)FeAsF. The temperature dependence of resistivity, magnetization, Hall effect, and magnetoresistance all exhibit quite similar behaviors as other parent compounds, but with the exception that the resistivity anomaly which was associated with the spin-density wave (SDW)/structural transition¹⁸ has not been found in present system up to 400 K. Superconductivity may be induced by doping electrons or holes in this compound.

II. EXPERIMENT

The compound Sr₃Sc₂O₅Fe₂As₂ was found while looking for iron arsenic analogs of materials with this structure type seen in related chemical systems.¹⁹ The polycrystalline samples were fabricated by using a two-step solid-state reaction method.²⁰ First, SrAs and ScAs powders were obtained by the chemical reaction method with Sr pieces, Sc pieces,

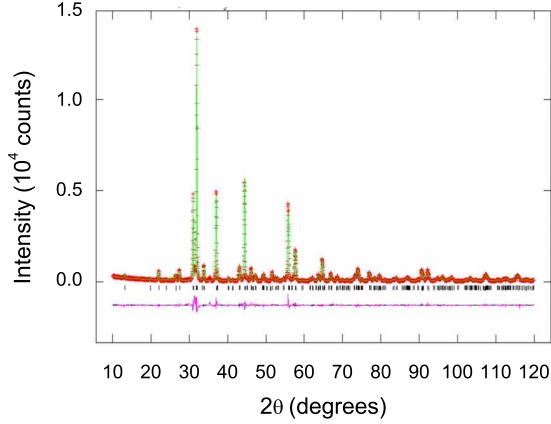


FIG. 1. (Color online) X-ray diffraction patterns and the Rietveld fit for the $(\text{Sr}_3\text{Sc}_2\text{O}_5)\text{Fe}_2\text{As}_2$ powder sample.

and As grains. Then they were mixed with Sc_2O_3 (purity 99.9%), SrO (purity 99%), Fe_2O_3 (purity 99.9%), and Fe powder (purity 99.9%) in the formula $(\text{Sr}_3\text{Sc}_2\text{O}_5)\text{Fe}_2\text{As}_2$, grounded and pressed into a pellet shape. The weighing, mixing, and pressing processes were performed in a glove box with a protective argon atmosphere (the H_2O and O_2 contents are both below 0.1 ppm). The pellets were sealed in a quartz tube with 0.2 bar of Ar gas and followed by a heat treatment at 1000 °C for 40 h. Then it was cooled down slowly to room temperature.

The x-ray diffraction (XRD) pattern of our samples was carried out by a *Mac-Science* MXP18A-HF equipment with $\theta-2\theta$ scan. The XRD data taken using powder sample was analyzed by the Rietveld fitting method using the GSAS suite.²¹ The starting parameters for the fitting were taken from isostructural $(\text{Sr}_3\text{Sc}_2\text{O}_5)\text{Cu}_2\text{S}_2$ and the program will finally find the best fitting parameters.¹⁹ The dc magnetization measurements were done with a superconducting quantum interference device (SQUID) (Quantum Design, MPMS7). For the magnetotransport measurements, the sample was shaped into a bar with the length of 3 mm, width of 2.5 mm, and thickness of about 0.8 mm. The resistance and Hall-effect data were collected using a six-probe technique on the Quantum Design instrument physical property measurement system (PPMS) with magnetic fields up to 9 T. The electric contacts were made using silver paste with the contacting resistance below 0.06 Ω at room temperature. The data acquisition was done using a dc mode of the PPMS, which measures the voltage under an alternative dc current and the sample resistivity is obtained by averaging these signals at each temperature. In this way the contacting thermal power is naturally removed. The temperature stabilization was better than 0.1% and the resolution of the voltmeter was better than 10 nV.

III. ANALYSIS TO THE STRUCTURAL DATA

The XRD pattern for the sample $(\text{Sr}_3\text{Sc}_2\text{O}_5)\text{Fe}_2\text{As}_2$ is shown in Fig. 1. One can see that the sample is very pure since no any visible peaks can be detected from the impurity phase. The data was well fitted with a single tetragonal

TABLE I. Fitting parameters, some angles (deg) for $(\text{Sr}_3\text{Sc}_2\text{O}_5)\text{Fe}_2\text{As}_2$. $wR_p=11.75\%$, $R_p=8.09\%$.

Atom	Site	x	y	Z	B	Angle (deg)
Sc	4e	0	0	0.07399(12)	0.28(6)	
Fe	4d	0.5	0	0.25	0.46(6)	
Sr	2b	0.5	0.5	0	1.2(5)	
Sr	4e	0.5	0.5	0.14006(6)	0.51(4)	
As	4e	0	0	0.20018(6)	0.62(4)	
O	8g	0.5	0	0.08323(23)	0.54(14)	
O	2a	0	0		0.82(31)	
α						113.30(7)
β						107.590(32)
γ						72.410(32)
δ						113.30(7)

$(\text{Sr}_3\text{Sc}_2\text{O}_5)\text{Fe}_2\text{As}_2$ phase with the space group of $I4/mmm$. Rietveld refinement shown by the solid line in the figure gives good agreement between the data and the calculated profiles. Lattice parameters for the tetragonal unit cell was determined to be $a=4.069$ Å and $c=26.876$ Å. In Table I, the structure parameters, angles of As-Fe-As and Fe-As-Fe (as marked in Fig. 2) were listed with agreement factors: $wR_p=11.75\%$, $R_p=8.09\%$.

It is clear that the a -axis lattice constant of this parent phase is slightly larger than that of the REFeAsO , $(\text{Ba},\text{Sr})\text{Fe}_2\text{As}_2$, and $(\text{Sr},\text{Ca},\text{Eu})\text{FeAsF}$ systems, while the c

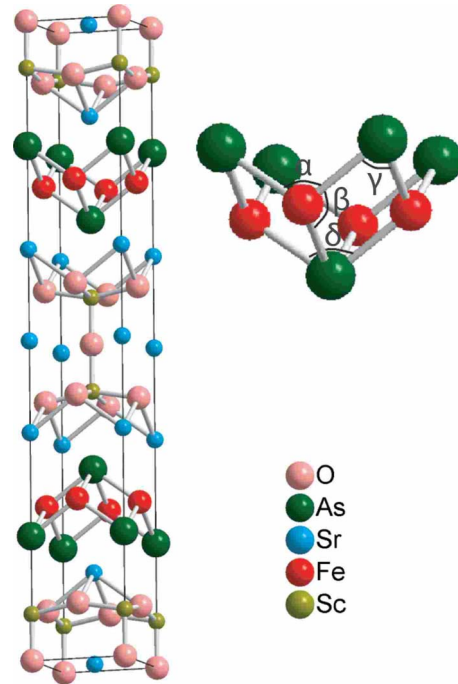


FIG. 2. (Color online) (Left) Crystal structure of $(\text{Sr}_3\text{Sc}_2\text{O}_5)\text{Fe}_2\text{As}_2$. Now the Fe_2As_2 layers are well separated by the building block $\text{Sr}_3\text{Sc}_2\text{O}_5$. (Right) An enlarged view about the FeAs block on which four different angles are marked: α : As-Fe-As (I), β : As-Fe-As (II), γ : Fe-As-Fe (I), and δ : Fe-As-Fe (II).

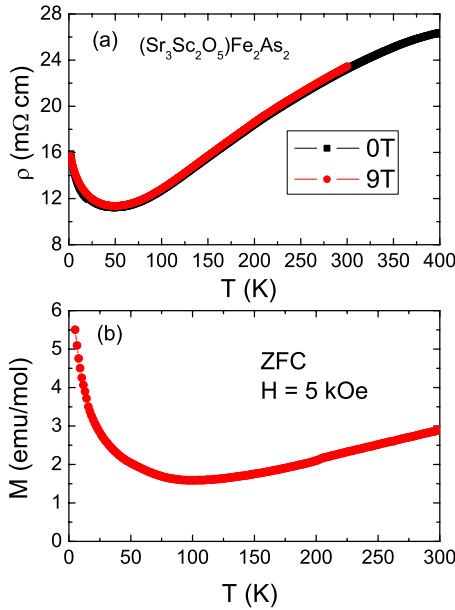


FIG. 3. (Color online) (a) Temperature dependence of resistivity for the $(\text{Sr}_3\text{Sc}_2\text{O}_5)\text{Fe}_2\text{As}_2$ sample at zero field up to 400 K and 9 T up to 300 K. A clear upturn in the low-temperature region can be seen. (b) Temperature dependence of dc magnetization for the zero-field cooling (ZFC) process at a magnetic field of $H=5000$ Oe.

axis one is much larger.^{1,13,20,22} The skeleton shown in the right-hand side of Fig. 2 gives the structure model of our sample. It is clear that the Fe ions construct a square lattice and the FeAs-layer stacks with the $(\text{Sr}_3\text{Sc}_2\text{O}_5)$ building block along c axis. The spacing distance between two neighboring FeAs layers of about 13.438 Å is much larger than those in all other FeAs-based compounds discovered so far, such as REFeAsO, $(\text{Ba},\text{Sr})\text{Fe}_2\text{As}_2$, and $(\text{Sr},\text{Ca},\text{Eu})\text{FeAsF}$. This may induce high T_c superconductivity by doping charges into the system. In fact, this kind of structures were reported and classified to the general formula $(\text{Cu}_2\text{S}_2)(\text{Sr}_{n+1}\text{M}_n\text{O}_{3n-1})$.¹⁹

IV. ELECTRICAL AND MAGNETIC PROPERTIES

In Fig. 3(a) we present the temperature dependence of resistivity for the $(\text{Sr}_3\text{Sc}_2\text{O}_5)\text{Fe}_2\text{As}_2$ sample under two magnetic fields 0 and 9 T. The data under zero field were collected in temperature region up to 400 K. A weak upturn in the low-temperature regime can be seen under both fields, representing a weak semiconductorlike behavior for the present sample. This behavior was attributed to the weak localization effect in our sample. Interestingly, the similar weak upturn of resistivity was observed in stoichiometric LaOFeP.²³ A metallic behavior can be seen in the temperature dependence of resistivity in the temperature regime above 60 K. Interestingly, no resistivity anomaly corresponding to the SDW transition was observed up to 400 K. This can be further confirmed by the magnetization data as shown in Fig. 3(b), which shows the zero-field cooled dc magnetization at 5000 Oe. Again no anomaly was observed in the magnetization data. This is rather different from other FeAs-based parent compounds, such as REFeAsO,¹ $(\text{Ba},\text{Sr})\text{Fe}_2\text{As}_2$

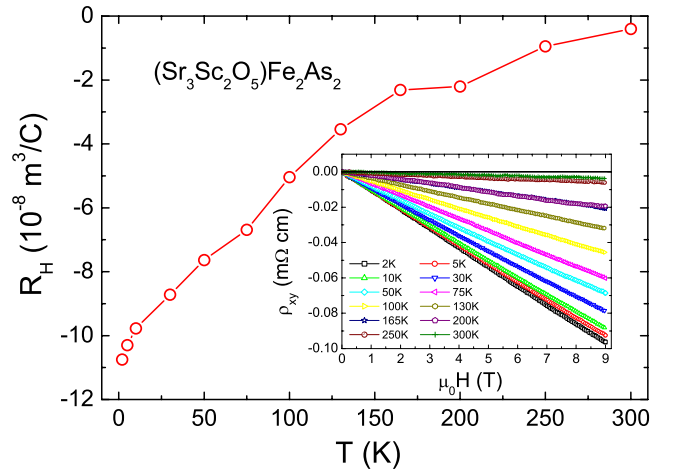


FIG. 4. (Color online) Temperature dependence of Hall coefficient R_H determined on the sample $(\text{Sr}_3\text{Sc}_2\text{O}_5)\text{Fe}_2\text{As}_2$. Negative values of R_H and a strong temperature dependence can be seen. Inset: the raw data of the Hall resistivity ρ_{xy} versus the magnetic field $\mu_0 H$ at different temperatures.

(Refs. 5 and 6) and $(\text{Sr},\text{Ca},\text{Eu})\text{FeAsF}$,¹³ where clear resistivity and magnetization anomaly associated with the SDW/structural transition have been observed. We attribute it to the rather large spacing distance between the neighboring FeAs layers in the present system, which prevents from forming the antiferromagnetic correlation between the moments of Fe ions in neighboring FeAs layers.

To further understand the conducting carriers in the present sample, we also carried out the Hall-effect measurements on the present sample. The inset of Fig. 4 shows the magnetic field dependence of Hall resistivity (ρ_{xy}) at different temperatures. In the experiment, ρ_{xy} was taken as $\rho_{xy} = [\rho(+H) - \rho(-H)]/2$ at each point to eliminate the effect of the misaligned Hall electrodes. It is clear that ρ_{xy} is negative at all temperatures below 300 K for $(\text{Sr}_3\text{Sc}_2\text{O}_5)\text{Fe}_2\text{As}_2$ leading to a negative Hall coefficient $R_H = \rho_{xy}/H$. This is similar to that of REFeAsO (Refs. 24 and 25) and $(\text{Ba},\text{Sr})\text{Fe}_2\text{As}_2$ parent phases, but in sharp contrast with $(\text{Sr},\text{Ca},\text{Eu})\text{FeAsF}$ in which the positive Hall coefficient R_H was found. The temperature dependence of the Hall coefficient R_H is presented in the main frame of Fig. 4. One can see that R_H remains negative in wide temperature regime up to 300 K and the absolute value of R_H decreases monotonically from 2 to 300 K. This indicates that electron-type charge carriers dominate the conduction in the present sample. The strong temperature dependent behavior of the Hall coefficient R_H suggests either a strong multiband effect or a spin related scattering effect. The absolute value of R_H is remarkably smaller than that of SrFeAsF system, indicating a relatively higher density of charge carriers.

The magnetoresistance (MR) is a very powerful tool to investigate the properties of electronic scattering.^{26,27} Field dependence of MR for the present sample at different temperatures is shown in the main frame of Fig. 5. One can see a systematic evolution of the curvature in the $\Delta\rho/\rho_0$ vs H curve, where $\Delta\rho = \rho(H) - \rho_0$, $\rho(H)$ and ρ_0 represents the longitudinal resistivity at a magnetic field H and that at zero field. The MR data at 2 K is positive with a hump shape

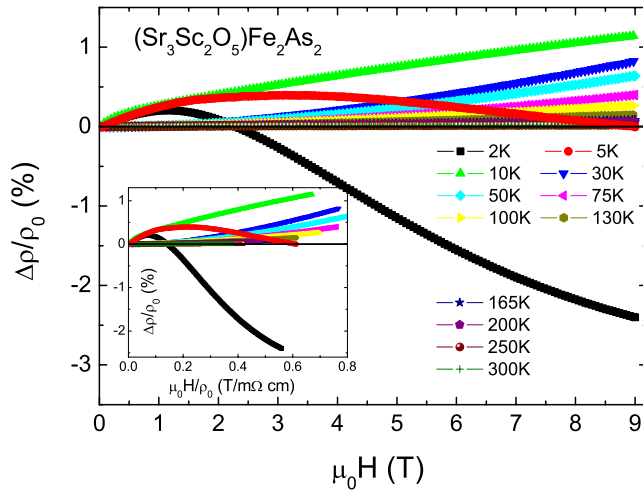


FIG. 5. (Color online) Field dependence of MR for the present sample at different temperatures is shown in the main frame. The inset shows the Kohler plot of MR. The MR is positive at a low field and turns to be negative at low temperatures.

below 2.3 T and becomes negative at higher fields. While at 5 K, a maximum value of MR appears at about 3.3 T and it decreases until becoming zero at 9 T. The data at 10 K have a downward curvature compared with that measured at higher temperatures. We attribute the complicated behavior at low temperatures, especially the negative MR effect at 2 K, to the Kondo effect which is associated very well with the upturn of resistivity or the magnetic susceptibility, or to the magnetic field induced delocalization effect. The semiclassical transport theory has predicted that Kohler's rule will be held if only one isotropic relaxation time is present in a solid-state system.²⁸ Kohler's rule can be written as

$$\frac{\Delta\rho}{\rho_0} = \frac{\rho(H) - \rho_0}{\rho_0} = F\left(\frac{H}{\rho_0}\right). \quad (1)$$

This equation means that the $\Delta\rho/\rho_0$ vs H/ρ_0 curves for different temperatures, the so-called Kohler's plot, should be

scaled to a universal curve if Kohler's rule is obeyed. The scaling based on the Kohler plot of our sample is revealed in the inset of Fig. 5. An obvious violation of Kohler's rule can be seen from this plot. This behavior may indicate a multi-band effect or a complicated scattering mechanism, such as the Kondo effect or the weak localization in the low-temperature region. This kind of upturn of resistivity and the magnetic susceptibility in the low-temperature limit seem to be common features for the parent phases of the FeAs-based compounds and further studies are certainly required to unravel the underlying physics.

V. CONCLUDING REMARKS

In summary, a parent phase of the FeAs-based family, $(\text{Sr}_3\text{Sc}_2\text{O}_5)\text{Fe}_2\text{As}_2$, with the space group of $I4/mmm$ was synthesized successfully using a two-step solid-state reaction method. Rather large spacing distance between the neighboring FeAs layers was found. No anomaly associated with the AF order was observed either in the data of temperature dependence of resistivity or dc magnetization, which was attributed to the rather large spacing distance between the neighboring FeAs layers. Strong Hall effect was observed in the temperature region up to 300 K. We found that the Hall coefficient R_H is negative in the entire temperature regime. We also observed a delocalization effect at low temperatures from the MR data. The violation of Kohler's rule along with the strong temperature dependence of R_H may suggest a multiband and/or a spin scattering effect in this system. By doping electrons or holes in this compound, superconductivity may be achieved.

ACKNOWLEDGMENTS

This work is supported by the Natural Science Foundation of China, the Ministry of Science and Technology of China (973 Projects No. 2006CB601000 and No. 2006CB921802), the Knowledge Innovation Project of Chinese Academy of Sciences (ITSNEM).

*hhwen@aphy.iphy.ac.cn

¹Y. Kamihara, T. Watanabe, M. Hirano, and H. Hosono, *J. Am. Chem. Soc.* **130**, 3296 (2008).

²Z. A. Ren, W. Lu, J. Yang, W. Yi, X. L. Shen, Z. C. Li, G. C. Che, X. L. Dong, L. L. Sun, F. Zhou, and Z. X. Zhao, *Chin. Phys. Lett.* **25**, 2215 (2008).

³C. Wang, L. Li, S. Chi, Z. Zhu, Z. Ren, Y. Li, Y. Wang, X. Lin, Y. Luo, S. Jiang, X. Xu, G. Cao, and X. Zhu'an, *Europhys. Lett.* **83**, 67006 (2008).

⁴Peng Cheng, Bing Shen, Gang Mu, Xiyu Zhu, Fei Han, Bin Zeng, and Hai-Hu Wen, arXiv:0812.1192 (unpublished).

⁵M. Rotter, M. Tegel, D. Johrendt, I. Schellenberg, W. Hermes, and R. Pöttgen, *Phys. Rev. B* **78**, 020503(R) (2008).

⁶M. Rotter, M. Tegel, and D. Johrendt, *Phys. Rev. Lett.* **101**, 107006 (2008).

⁷K. Sasmal, B. Lv, B. Lorenz, A. M. Guloy, F. Chen, Y. Y. Xue,

and C. W. Chu, *Phys. Rev. Lett.* **101**, 107007 (2008).

⁸X. C. Wang, Q. Q. Liu, Y. X. Lv, W. B. Gao, L. X. Yang, R. C. Yu, F. Y. Li, and C. Q. Jin, *Solid State Commun.* **148**, 538 (2008).

⁹Joshua H. Tapp, Zhongjia Tang, Bing Lv, Kalyan Sasmal, Bernd Lorenz, Paul C. W. Chu, and Arnold M. Guloy, *Phys. Rev. B* **78**, 060505(R) (2008).

¹⁰M. J. Pitcher, D. R. Parker, P. Adamson, S. J. C. Herkelrath, A. T. Boothroyd, and S. J. Clarke, *Chem. Commun. (Cambridge)* **2008**, 5918.

¹¹F.-C. Hsu, J.-Y. Luo, K.-W. Yeh, T.-K. Chen, T.-W. Huang, P. M. Wu, Y.-C. Lee, Y.-L. Huang, Y.-Y. Chu, D.-C. Yan, and M.-K. Wu, *Proc. Natl. Acad. Sci. U.S.A.* **105**, 14262 (2008).

¹²T. Klimczuk, T. M. McQueen, A. J. Williams, Q. Huang, F. Ronning, E. D. Bauer, J. D. Thompson, M. A. Green, and R. J. Cava, arXiv:0808.1557 (unpublished).

- ¹³Fei Han, Xiyu Zhu, Gang Mu, Peng Cheng, and Hai-Hu Wen, Phys. Rev. B **78**, 180503(R) (2008).
- ¹⁴M. Tegel, S. Johansson, V. Weiss, I. Schellenberg, W. Hermes, R. Poettgen, and Dirk Johrendt, EPL **84**, 67007 (2008).
- ¹⁵S. Matsuishi, I. Yasunori, T. Nomura, H. Yanagi, M. Hirano, and H. Hosono, J. Am. Chem. Soc. (to be published).
- ¹⁶X. Y. Zhu, F. Han, P. Cheng, G. Mu, B. Shen, and H. H. Wen, arXiv:0810.2531 (unpublished).
- ¹⁷For the structures of different families of cuprate superconductors, see for example D. Hohlwein, *Materials and Crystallographic Aspects of High-T_c Superconductivity*, NATO ASI Series E: Applied Sciences, edited by E. Kaldis (Kluwer, Dordrecht, 1994), Vol. 263, p. 16, and references therein.
- ¹⁸Clarina de la Cruz, Q. Huang, J. W. Lynn, Jiying Li, W. Ratcliff II, J. L. Zarestky, H. A. Mook, G. F. Chen, J. L. Luo, N. L. Wang, and Pengcheng Dai, Nature (London) **453**, 899 (2008).
- ¹⁹K. Otszchi, H. Ogino, S. Jun-ichi, and K. Kishio, J. Low Temp. Phys. **117**, 729 (1999).
- ²⁰X. Zhu, H. Yang, L. Fang, G. Mu, and H.-H. Wen, Supercond. Sci. Technol. **21**, 105001 (2008).
- ²¹AC Larson, RB Von Dreele, General Structure Analysis System (GSAS), Los Alamos National Laboratory Report LAUR 86-748, 2000, (unpublished).
- ²²N. Ni, S. L. Bud'ko, A. Kreyssig, S. Nandi, G. E. Rustan, A. I. Goldman, S. Gupta, J. D. Corbett, A. Kracher, and P. C. Canfield, Phys. Rev. B **78**, 014507 (2008).
- ²³T. M. McQueen, M. Regulacio, A. J. Williams, Q. Huang, J. W. Lynn, Y. S. Hor, D. V. West, M. A. Green, and R. J. Cava, Phys. Rev. B **78**, 024521 (2008).
- ²⁴P. Cheng, H. Yang, Y. Jia, L. Fang, X. Zhu, G. Mu, and H.-H. Wen, Phys. Rev. B **78**, 134508 (2008).
- ²⁵A. S. Sefat, M. A. McGuire, B. C. Sales, R. Jin, J. Y. Howe, and D. Mandrus, Phys. Rev. B **77**, 174503 (2008).
- ²⁶Q. Li, B. T. Liu, Y. F. Hu, J. Chen, H. Gao, L. Shan, H. H. Wen, A. V. Pogrebnnyakov, J. M. Redwing, and X. X. Xi, Phys. Rev. Lett. **96**, 167003 (2006).
- ²⁷H. Yang, Y. Liu, C. G. Zhuang, J. R. Shi, Y. G. Yao, S. Massidda, M. Monni, Y. Jia, X. X. Xi, Q. Li, Z. K. Liu, Q. R. Feng, and H. H. Wen, Phys. Rev. Lett. **101**, 067001 (2008).
- ²⁸J. M. Ziman, *Electrons and Phonons, Classics Series* (Oxford University Press, New York, 2001).